TOXICOLOGICAL SCIENCES **118(2)**, 554–563 (2010)
doi:10.1093/toxsci/kfq305
Advance Access publication October 8, 2010

Aryl Hydrocarbon Receptor Nuclear Translocator in Hepatocytes Is Required for Aryl Hydrocarbon Receptor–Mediated Adaptive and Toxic Responses in Liver

Manabu Nukaya,*,† Jacqueline A. Walisser,* Susan M. Moran,* Gregory D. Kennedy,† and Christopher A. Bradfield*,[1]

*McArdle Laboratory for Cancer Research and †Department of Surgery, University of Wisconsin School of Medicine and Public Health, Madison, Wisconsin 53706

[1]To whom correspondence should be addressed. Fax: (608) 262-2824. E-mail: bradfield@oncology.wisc.edu.

Received August 3, 2010; accepted September 25, 2010

The aryl hydrocarbon receptor (AHR) plays a central role in the toxic responses to halogenated dibenzo-*p*-dioxins ("dioxins"), in the metabolic adaptation to polycyclic aromatic hydrocarbons, and in the development of the mature vascular system. A number of lines of evidence support the idea that the regulation of adaptive metabolism requires an AHR partnership with the aryl hydrocarbon receptor nuclear translocator (ARNT). Yet, for AHR-dependent vascular development and dioxin toxicity, the role of ARNT is less certain. In fact, numerous models have been proposed over the years to suggest that the AHR signals in important ways via ARNT-independent events. In an effort to clarify the role of ARNT in AHR-mediated dioxin hepatotoxicity, we generated a conditional *Arnt* mouse model. Such a model was essential because global inactivation of *Arnt* results in embryonic lethality presumably due to this protein's role as a heterodimeric partner for the hypoxia-inducible factors (HIFs). Using a hepatocyte-specific *Arnt* deletion, we were able to demonstrate that hepatocyte ARNT is required for major aspects of AHR-mediated dioxin toxicity in the liver. Results from this conditional *Arnt* allele are also consistent with a model where hepatocyte ARNT is unrelated to AHR-mediated hepatovascular development. In sum, these data suggest that AHR-ARNT dimers within the hepatocyte direct the toxic and adaptive and developmental functions associated with the AHR and that developmental vascular events arise due to signaling in a distinct cell type expressing this dimeric pair.

Key Words: **AHR; ARNT; dioxin; liver toxicity; hepatocyte.**

The aryl hydrocarbon receptor (AHR) and aryl hydrocarbon receptor nuclear translocator (ARNT) are founding members of the basic helix-loop-helix/Per-Arnt-Sim (PAS) superfamily of transcription factors (McIntosh *et al*., 2010). These proteins are central components of a signaling pathway originally identified for its role in regulating the adaptive metabolic responses to a variety of environmental pollutants (Hankinson, 1995; Schmidt and Bradfield, 1996). In the most common depiction of signaling, the AHR binds xenobiotics with extended aromatic structure and the AHR then translocates into the nucleus where it forms a heterodimeric complex with the ARNT protein. This AHR-ARNT nuclear complex recognizes dioxin-responsive enhancer elements (DREs) found upstream of target genes (Hankinson, 1995; Schmidt and Bradfield, 1996). The resultant AHR-ARNT-DRE interactions lead to the upregulation of genes encoding both phase I and phase II xenobiotic metabolism enzymes (e.g., the *Cyp1a1*, *Cyp1a2*, *Cyp1b1*, and the *Gst-ya* genes) (Hankinson, 1995; Nebert and Gonzalez, 1987; Schmidt and Bradfield, 1996).

In addition to its role in the adaptive metabolism of polycyclic aromatics, the AHR also plays additional roles in mammalian biology. In this regard, the AHR has long been known to mediate toxic responses to certain halogenated dibenzo-*p*-dioxins, such as 2,3,7,8-tetrachlorodibenzo-*p*-dioxin (dioxin) (Pohjanvirta and Tuomisto, 1994). Receptor-mediated dioxin end-points include tumor promotion, chloracne, thymic involution, teratogenesis, and hepatotoxicity (Pohjanvirta and Tuomisto, 1994). More recently, the AHR has been studied for its potential role in normal physiology. Studies with *Ahr* null and mutant alleles have revealed a role for this receptor in a number of vascular remodeling events, including the developmental closure of a hepatovascular portocaval shunt known as the "ductus venosus" (DV) (Harstad *et al*., 2006; Lahvis *et al*., 2000).

In our efforts to understand the role of the AHR in each of these distinct biological response pathways, we have employed several *Ahr* mutant mouse models. For example, mice harboring *Ahr* null and hypomorphic alleles have been used to demonstrate that the AHR is essential for adaptive xenobiotic metabolism, dioxin toxicity, and normal hepatovascular development (Lahvis *et al*., 2000; Walisser *et al*., 2004a). Moreover, "knock-in" alleles have been used to create mice harboring mutations in either the DRE binding or the nuclear localization motifs of the AHR protein (Bunger *et al*., 2003, 2008). These models have supported the idea that the developmental, adaptive, and toxic responses all require the

nuclear translocation and DNA-binding properties of AHR. Finally, a conditional *Ahr* null allele allowing excision of this gene in either hepatocytes or endothelial cells has provided evidence that the AHR in hepatocytes is necessary to produce the adaptive and toxic responses of dioxin exposure in liver, whereas the AHR in endothelial cells plays the more significant role for the hepatovascular development (Walisser *et al*., 2005).

Understanding the role of ARNT in the various aspects of AHR biology is an important topic. In recent years, a number of laboratories have provided evidence of AHR-mediated signaling events that are ARNT independent (Ge and Elferink, 1998; Klinge *et al*., 2000; Oesch-Bartlomowicz *et al*., 2005; Puga *et al*., 2000; Reiners and Clift, 1999; Seidel and Denison, 1999; Tian *et al*., 1999; Vogel *et al*., 2007; Weiss *et al*., 2008). Moreover, identification of the PAS protein, known as ARNT2, has also led to the suggestion that this paralogue may provide a unique dimerization partner for the AHR that could direct signaling in a cell-specific manner (Dougherty and Pollenz, 2008; Hirose *et al*., 1996). Understanding the role of ARNT in AHR signaling is complicated by the fact that ARNT is also a partner of other PAS proteins, including the hypoxia-inducible factors (HIFs) (McIntosh *et al*., 2010). Because of this role in HIF signaling, *Arnt* null animals die in early development due to early blocks in embryonic angiogenesis (Kozak *et al*., 1997; Maltepe *et al*., 1997). In previous work, our laboratory generated *Arnt* hypomorphic mice that express ~10% of normal ARNT protein (Walisser *et al*., 2004b). This hypomorphic mouse develops through the HIF-dependent development stages, yet displays the patent DV similar to the *Ahr* null allele (Walisser *et al*., 2004b). This finding supports the idea that the AHR-ARNT dimer drives the closure of the DV during later stages of liver development. Unfortunately, the *Arnt* null and hypomorphic models have less utility when trying to define the role for ARNT in AHR-mediated dioxin toxicity. In this regard, the early embryonic lethality of the global *Arnt* null mice prevents study of any late stage developmental or postnatal end points, and the high frequency of patent DV in the hypomorphic *Arnt* allele leads to uncertainties with respect to the disposition of hepatotoxicants-like dioxin.

In an effort to understand the role for the ARNT protein in the AHR-mediated toxicity of compounds like dioxin, we developed a hepatocyte-specific null allele of *Arnt* that bypassed the embryonic lethality of the global *Arnt* null and the hepatovascular and HIF-dependent defects dependent upon ARNT expression in the endothelial cell component. By using this hepatocyte-specific *Arnt* deletion mouse model, we show that ARNT in hepatocytes is a primary component of the liver's adaptive metabolic response and dioxin-induced hepatotoxic response.

EXPERIMENTAL PROCEDURES

Generation of conditional* Arnt$^{fx/fx}$ *mice. To generate the conditional *Arnt*$^{fx/fx}$ (fx; flanked by *lox-p* sites or "floxed") mice, we used mice harboring the hypomorphic *Arnt* allele (designated *Arnt*^{fxneo}) (Fig. 1A) (Walisser *et al*., 2004b). For heritable excision of the neomycin-resistant cassette (*Neo*), the *Arnt*$^{fxneo/+}$ mice were crossed to mice carrying *Cre*^{EIIa} transgene (*Cre*^{EIIa}; strain name: FVB_N-Tg (EIIa-cre) C5379Lmgd_J) (The Jackson Laboratory, Bar Harbor, ME) (Lakso *et al*., 1996). The excision of the *Neo* was confirmed by PCR genotyping. The PCR was performed by using three primers (OL5287: 5′-GGCCGTTTCTCACATGAAGT-3′, OL6021: 5′-TGCCTGCTCTTTACTGAAGGC-3′, and OL5288: 5′-GGAGCAACAGGGGTTGTTTA-3′). The PCR was carried out for 30 cycles (95°C for 30 s, 59°C for 45 s, and 72°C for 45 s) in a reaction mixture containing 2.5 U of *Taq* polymerase (Promega, Madison, WI), 50mM KCl, 10mM Tris-HCl (pH 9.0 at 25°C), 1.5mM $MgCl_2$, 1% Triton X-100, 0.2mM dNTPs, and 0.2μM each primer. The obtained 571-, 736-, and 604-bp PCR products corresponded to *Arnt*$^{+}$, *Arnt*^{fxneo}, and *Arnt*^{fx} alleles, respectively. The resultant *Arnt*$^{fx/+}$ mice were backcrossed to C57BL/6J mice for four generations. Following the backcross, the progeny were interbred to generate homozygous *Arnt*$^{fx/fx}$ mice.

Generation of hepatocyte-specific* Arnt *null mice. To generate mice harboring the *Arnt* null allele in hepatocytes, the conditional *Arnt*$^{fx/fx}$ mice were crossed to *Cre*^{alb} mice expressing Cre recombinase in hepatocytes (*Cre*^{alb}; strain name: B6.Cg-Tg(Albcre) 21Mgn_J) (The Jackson Laboratory) (Fig. 1A) (Postic *et al*., 1999). To obtain hepatocyte-specific *Arnt* null mice (*Arnt*$^{fx/fx}$*Cre*^{alb}), the *Arnt*$^{fx/+}$*Cre*^{alb} mice were crossed to homozygous *Arnt*$^{fx/fx}$ mice. The excision of exon 6 flanked by *lox-p* sites was confirmed by using three PCR primers (OL5287, OL5288, and OL2300: 5′-GCAACTTTGACAAGGCAGCATTTA-3′). These primers amplified a 571-, 604- and 441-bp bands from the genome of *Arnt*$^{+}$, *Arnt*^{fx}, and *Arnt* null alleles, respectively. All strains of mice were selected for homozygosity for the *AHR*^{b1} allele (Nukaya *et al*., 2009).

Animals and toxicology studies. Mice were housed in a selective pathogen-free facility on corncob bedding with food and water *ad libitum* following the protocol established by University of Wisconsin Medical School Animal Care and Use Committee. The *Cre*^{EIIa} and *Cre*^{alb} mice were backcrossed to C57BL/6J mice for > 10 generation prior to use in these experiments. Seven-week-old male mice were injected with a single intraperitoneal (ip) dose of 2,3,7,8-tetrachlorodibenzo-*p*-dioxin (100 μg/kg total body weight) dissolved in dimethyl sulfoxide (DMSO) or DMSO alone. Seven days after the single intraperitoneal (ip) injection, mice were sacrificed by CO_2 euthanasia (Walisser *et al*., 2005). Serum samples were prepared and alanine aminotransferase (ALT) activity was measured as described previously (Nukaya *et al*., 2009). Liver, lung, kidney, heart, spleen, and thymus were removed and weighed. Liver samples were used for preparation of total RNA, microsomal and cytosolic proteins, and for histology (Nukaya *et al*., 2009). The left liver lobe was sliced and fixed in 10% (vol/vol) formalin in PBS or embedded in frozen section compound (Surgipath,

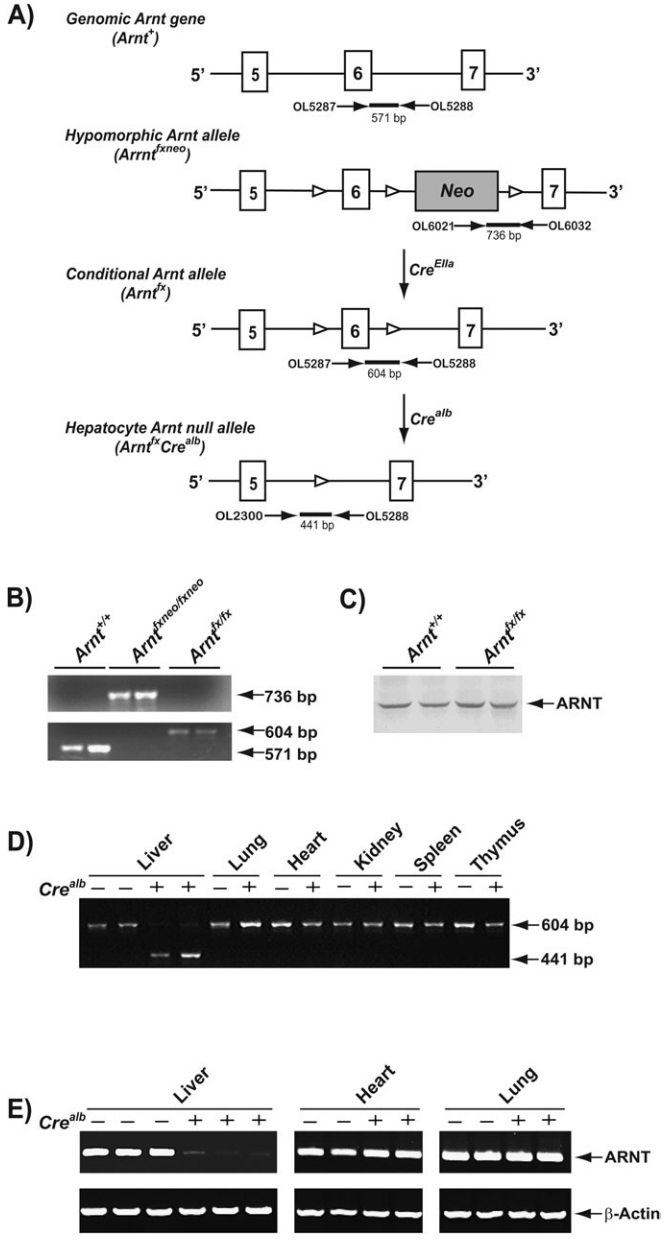

FIG. 1. Generation of hepatocyte-*Arnt* null mice. (A) Targeting strategy and genome maps of native mouse *Arnt* gene ($Arnt^{+}$), hypomorphic *Arnt* allele ($Arnt^{fxneo}$), conditional *Arnt* allele ($Arnt^{fx}$), and hepatocyte-*Arnt* null allele ($Arnt^{fx}Cre^{alb}$). The closed boxes indicate exons of mouse *Arnt* gene (exons 5–7). Open arrowhead, *lox-P* site. (B) Genotyping for wild-type ($Arnt^{+}$), $Arnt^{fxneo}$, and $Arnt^{fx}$ allele. The 571-, 736, and 604-bp bands were corresponded to $Arnt^{+}$, $Arnt^{fxneo}$, and $Arnt^{fx}$ alleles, respectively. (C) Comparison of hepatic ARNT protein levels between $Arnt^{+/+}$ and $Arnt^{fx/fx}$ mice. Cytosolic proteins were isolated from the liver of $Arnt^{+/+}$ and $Arnt^{fx/fx}$ mice. One hundred micrograms of cytosolic extracts were analyzed by Western blot analysis using mouse ARNT-specific antibody. (D) PCR genotyping for $Arnt^{fx/fx}$ and *Arnt* $Arnt^{fx/fx}Cre^{alb}$ mice. Genomic DNA was extracted from individual tissue from $Arnt^{fx/fx}$ ($Cre^{alb}(-)$) and $Arnt^{fx/fx}Cre^{alb}$ ($Cre^{alb}(+)$) mice. The 604- and 441 bp-amplified bands were corresponded to $Arnt^{fx}$ and *Arnt* null alleles, respectively. (E) Comparison of ARNT mRNA levels between $Arnt^{fx/fx}$ and $Arnt^{fx/fx}Cre^{alb}$ mice. The ARNT and β-actin mRNA levels were detected by RT-PCR. Total RNA was extracted from individual tissue (liver, heart, and lung) from $Arnt^{fx/fx}$ ($Cre^{alb}(-)$), and $Arnt^{fx/fx}Cre^{alb}$ ($Cre^{alb}(+)$) mice.

Richmond, IL). Paraffin-embedded sections were stained with hematoxylin and eosin (H&E) and immunostained with anti-F4/80 antibody. Frozen sections were stained with Oil Red O, as described previously (Nukaya *et al.*, 2009).

Assessment of DV status. The status of the DV was confirmed by perfusion of the liver with 0.4% trypan blue, as described previously (Nukaya *et al.*, 2009; Walisser *et al.*, 2005). The hypomorphic $Arnt^{fxneo/fxneo}$ mice were employed as positive controls for DV patency (Walisser *et al.*, 2004b).

Gene expression analysis. Total RNA was isolated by using the Qiagen RNeasy Kit (Qiagen, Valencia, CA). The ARNT messenger RNA (mRNA) level was determined by reverse transcriptase PCR (RT-PCR). Briefly, 3 μg of total RNA extracted from liver, lung, and heart was reverse transcribed with 2 ng of random $p(dN)_6$ primer (Roche, Indianapolis, IN), 20 U of RNase inhibitor (Promega), 0.4mM dNTPs mixture (Promega), and 25 U of AMV-reverse transcriptase (Roche). The synthesized complementary DNAs (cDNAs) were mixed with a reaction mixture containing 2.5 U of *Taq* polymerase (Promega), 50mM KCl, 10mM Tris-HCl, 1.5mM $MgCl_2$, 1% Triton X-100, 0.2mM dNTPs, and 0.2μM primers. The PCR was carried out for 28 cycles (95°C for 10 s, 58°C for 30 s, and 72°C for 30 s) by using mouse ARNT and β-actin mRNA-specific PCR primers (ARNT mRNA [F], 5′-GCACACAGAACTGGATATGGTACC-3′; ARNT mRNA [R], 5′-AGGGGTAAGACCACTATTCCTGA-3′; β-actin mRNA [F], 5′-ATGAAGTGTGACGTTGACATCCG-3′; and β-actin mRNA [R], 5′-GCTTGCTGATCCACATCTGCTG-3′). The PCR products were subjected to electrophoresis on a 2% agarose gel and then visualized by ethidium bromide staining. The β-actin mRNA level was used as internal control.

The mRNA levels of *Cyp1a1*, *Cyp1a2*, *Cyp1b1*, and *Ahrr* were measured by using northern blot analysis and quantitative RT-PCR. For the northern blot analysis, 10 μg of total RNA was loaded upon 0.8% agarose gels containing 18% formaldehyde and transferred to Hybond-N+ membrane (GE Healthcare Bio-Science, Piscataway, NJ). The membrane was hybridized with ^{32}P-labeled cDNA probes for detection of *Cyp1a1*, *Cyp1a2*, *Cyp1b1*, and *Gapdh* mRNA as previously described (Nukaya *et al.*, 2009; Walisser *et al.*, 2005). For the quantitative RT-PCR, total RNA was reverse transcribed using the High-Capacity cDNA Reverse Transcription Kit (Applied Biosystems, Foster City, CA). Expression levels of AHR-driven genes were measured with TaqMan Universal PCR Master Mix (Applied Biosystems) and custom-designed probes (Assay ID: *Cyp1a1*; Mm00487218_m1, *Cyp1a2*; Mm00487224_m1, *Cyp1b1*; Mm00487229_m1, *Ahrr*; Mm00477445_m1, *β-actin*; Mm01205647_g1). The GAPDH and β-actin mRNA levels were measured as internal controls.

Protein assays. Liver cytosolic and microsomal proteins were prepared as described previously (Nukaya *et al.*, 2009;

Walisser *et al*., 2004b). For Western blot analysis, 100 μg of cytosolic protein or 50 μg of microsomal protein was loaded onto SDS-polyacrylamide gels, electrophoresed, and transferred to Immobilon-P transfer membrane (Millipore, Bedford, MA). To ensure equal loading of all lanes, each membrane was stained with Ponceau S staining solution (Sigma-Aldrich, St Louis, MO) prior to incubation with Western blot reagents. For immunochemical detection, the membrane was incubated with ARNT, cytochrome P450 1A1 (CYP1A1), CYP1A2, CYP1B1, and β-actin antibodies (Nukaya *et al*., 2009; Savas *et al*., 1994; Walisser *et al*., 2004b). The bands were visualized using NBT/BCIP solution (Roche). The microsomal proteins were used for measurement of ethoxyresorufin-*O*-deethylase (EROD) and methoxyresorufin-*O*-deethylase (MROD) activities as described previously (Nukaya *et al*., 2009).

Statistical analysis. All statistical data are presented as mean ± SEM. Intergroup comparisons were performed by one-way ANOVA (Nukaya *et al*., 2009). Differences among groups were assessed statistically significant when the p value was < 0.05. Statistical analysis of genotype distribution was compared by χ^2 analysis.

RESULTS

Generation of Conditional Arnt$^{fx/fx}$ *Mice*

To obtain mice harboring the conditional *Arnt*^{fx} allele, heterozygous hypomorphic *Arnt* mice (*Arnt*$^{fxneo/+}$) were crossed to mice expressing *Cre* recombinase under control of the adenovirus *EIIa* promoter (*Cre*^{EIIa}), causing excision of the neomycin-resistant cassette (*Neo*) (Fig. 1A). Following heritable excision of *Neo*, the resultant mice were backcrossed to C57BL/6J mice to exclude the *Cre*^{EIIa} transgene. Excision of *Neo* was confirmed by PCR genotyping (Fig. 1B). The resulting progeny were interbred to obtain homozygous conditional *Arnt*$^{fx/fx}$ mice. In liver of the *Arnt*$^{fx/fx}$ mice, the ARNT protein levels were not significantly different compared with the *Arnt*$^{+/+}$ mice (Fig. 1C). The *Arnt*$^{fx/fx}$ mice were born in normal numbers and displayed normal development and were indistinguishable from the *Arnt*$^{+/+}$ mice.

Generation of Hepatocyte-Specific Arnt *Null (*Arnt$^{fx/fx}$Cre^{alb}*) Mice*

To obtain mice carrying the *Arnt* null allele in hepatocytes, the *Arnt*$^{fx/fx}$ mice were crossed to mice expressing *Cre* recombinase under control of the albumin promoter (*Cre*^{alb}) (Fig. 1A). The resultant heterozygous hepatocyte-specific *Arnt* null mice (*Arnt*$^{fx/+}$*Cre*^{alb}) were backcrossed to the *Arnt*$^{fx/fx}$ mice, and homozygous hepatocyte-specific *Arnt* null mice (*Arnt*$^{fx/fx}$*Cre*^{alb}) were generated. The *Arnt*$^{fx/fx}$*Cre*^{alb} mice were bred with the *Arnt*$^{fx/fx}$ mice and the offspring were employed in experiments. The hepatocyte-specific excision of exon 6 of the *Arnt* gene was confirmed by PCR genotyping of genomic DNA extracted from liver, lung, heart, kidney, spleen, and thymus (Fig. 1D). Only in livers of *Arnt*$^{fx/fx}$*Cre*^{alb} mice, was the *Arnt* null allele observed (i.e., excision of exon 6; Fig. 1D). Genotyping analysis of progeny indicated that the birth ratio of *Arnt*$^{fx/fx}$ and *Arnt*$^{fx/fx}$*Cre*^{alb} mice was consistent with simple Mendelian segregation of a viable allele (i.e., *Arnt*$^{fx/fx}$; 52% [56/108], *Arnt*$^{fx/fx}$*Cre*^{alb}; 48% [52/108] [$\chi^2 = 0.700$]. Semi-quantitative RT-PCR revealed that ARNT mRNA levels were selectively reduced in the livers of *Arnt*$^{fx/fx}$*Cre*^{alb} mice (Fig. 1E). Outward phenotypes, including male/female ratio and fertility were not significantly different between *Arnt*$^{fx/fx}$ and *Arnt*$^{fx/fx}$*Cre*^{alb} mice (data not shown).

The Arnt$^{fx/fx}$Cre^{alb} *Mice Display Normal Hepatic Vascular Development*

To investigate the role of hepatocyte ARNT on liver vascular development, we perfused the portal vein with trypan blue dye and monitored flow through the parenchyma (closed DV) or directly through to the "vena cava" (patent DV) (Nukaya *et al*., 2009; Walisser *et al*., 2005). All *Arnt*$^{fx/fx}$ mice and *Arnt*$^{fx/fx}$*Cre*^{alb} mice displayed normal flow (0% frequency of patent DV, respectively), whereas hypomorphic *Arnt* mice (*Arnt*$^{fxneo/fxneo}$), used as a positive control, showed 71% frequency of DV patency (Table 1) (Walisser *et al*., 2004b).

The Arnt$^{fx/fx}$Cre^{alb} *Mice Lose AHR-Mediated Adaptive Response in Liver*

To assess effect of hepatocyte-specific ARNT deletion in AHR-mediated adaptive response, we used northern blot analysis to measure the mRNA levels of AHR-responsive gene battery members (i.e., *Cyp1a1*, *Cyp1a2*, and *Cyp1b1*) in liver, lung, and heart of the *Arnt*$^{fx/fx}$ and *Arnt*$^{fx/fx}$*Cre*^{alb} mice after treatment of DMSO or dioxin (Figs. 2A and 2B). In livers of dioxin-treated *Arnt*$^{fx/fx}$*Cre*^{alb} mice, the significant induction of *Cyp1a1*, *Cyp1a2*, and *Cyp1b1* mRNA levels was not observed, whereas the dioxin-treated *Arnt*$^{fx/fx}$ mice displayed the induction of AHR-driven gene expression (Fig. 2A). In contrast to liver, the increase of *Cyp1a1* mRNA levels in lung and heart was not significantly different between the *Arnt*$^{fx/fx}$ and *Arnt*$^{fx/fx}$*Cre*^{alb} mice (Fig. 2B). In addition, we measured the mRNA levels of *Cyp1a1*, *Cyp1a2*, *Cyp1b1*, and *Ahrr* in the livers of the *Arnt*$^{fx/fx}$ and *Arnt*$^{fx/fx}$*Cre*^{alb} mice by employing

TABLE 1
Rate of DV Patency in *Arnt*$^{fx/fx}$, *Arnt*$^{fx/fx}$*Cre*^{alb}, and *Arnt*$^{fxneo/fxneo}$ Mice

Genotype	Patent DV (%)	N^a
Arnt$^{fx/fx}$	0	0/14
Arnt$^{fx/fx}$*Cre*^{alb}	0	0/15
Arnt$^{fxneo/fxneo}$	71	5/7

[a] N = number of animals with DV/total animals.

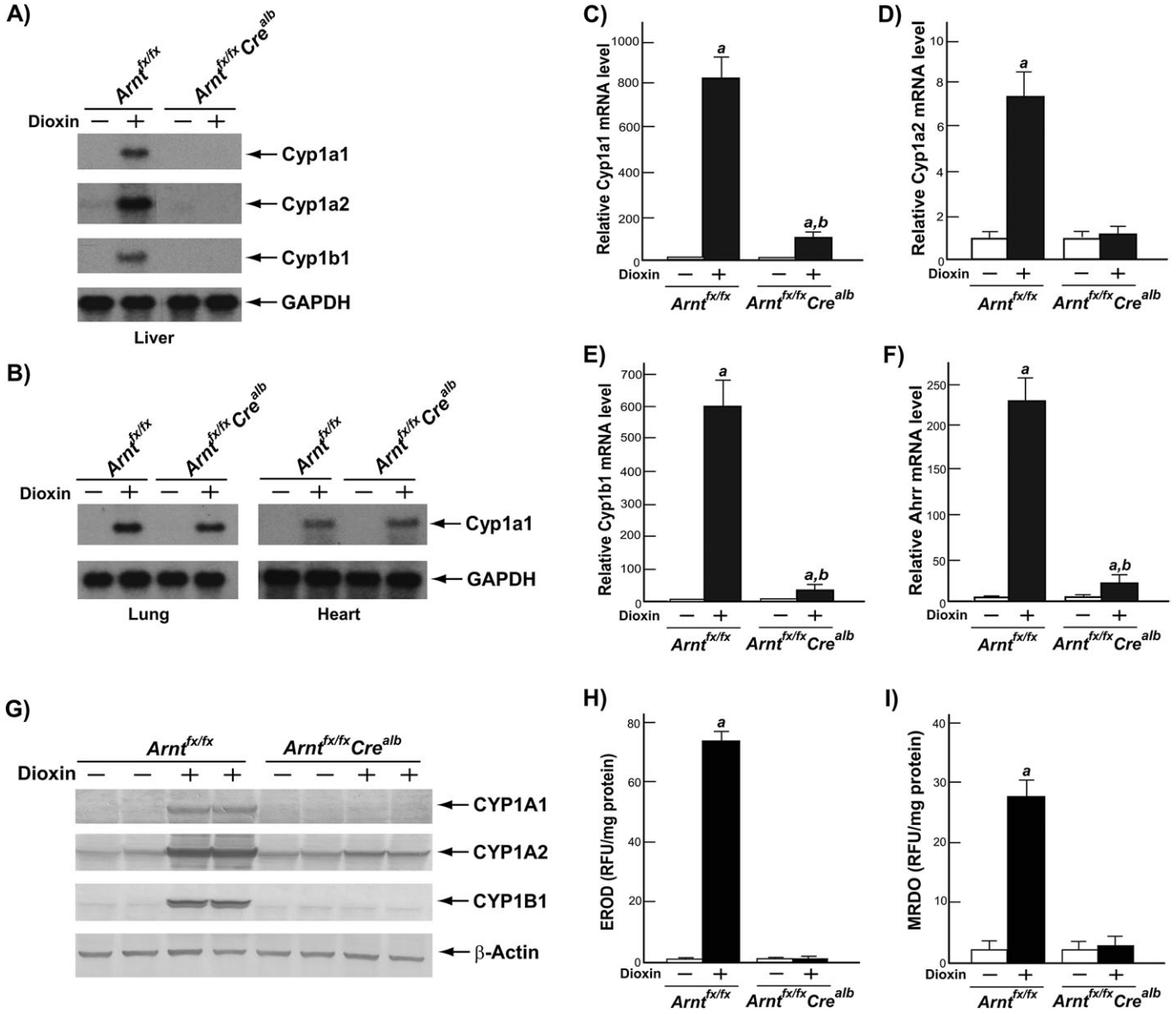

FIG. 2. Disruption of AHR-mediated adaptive response in the livers of $Arnt^{fx/fx}Cre^{alb}$ mice. Mice were treated with DMSO or 100 μg/kg of dioxin and sacrificed 7 days after the single ip injection. Total RNA was isolated from liver, lung, and heart of the $Arnt^{fx/fx}$ and $Arnt^{fx/fx}Cre^{alb}$ mice. (A and B) Induction of AHR gene batteries in liver (A) and lung and heart (B). The *Cyp1a1*, *Cyp1a2*, *Cyp1b1*, and *gapdh* mRNA were detected by northern blot analysis. (C–F) Relative fold induction of AHR gene batteries in liver (C) *Cyp1a1* mRNA, (D) *Cyp1a2* mRNA, (E) *Cyp1b1* mRNA, and (F) *Ahrr* mRNA. The mRNA levels of each gene were determined by quantitative RT-PCR, and these measured mRNA levels were normalized to β-actin mRNA levels. Results were expressed as relative mRNA level compared with DMSO-treated $Arnt^{fx/fx}$ mice. Each group contained four to six mice. Open bars, DMSO treatment; closed bars, dioxin treatment. Error bars represent SE a, significantly different relative to the DMSO-treated $Arnt^{fx/fx}$ mice ($p < 0.05$) and b, significantly different relative to the dioxin-treated $Arnt^{fx/fx}$ mice ($p < 0.05$). (G–I) Microsomal proteins were isolated from the livers of $Arnt^{fx/fx}$ and $Arnt^{fx/fx}Cre^{alb}$ mice. (G) Fifty micrograms of microsomal extracts were analyzed by Western blot analysis using mouse CYP1A1, CYP1A2, CYP1B1, and β-actin antibodies. (H) EROD (CYP1A1 enzyme activity) and (I) MROD (CYP1A2 activity). These activities are expressed as RFU (Relative Fluorescence Units) per milligram of microsomal protein. Each group contained four to six mice. Open bars, DMSO treatment; closed bars, dioxin treatment. Error bars represent SE a, significantly different relative to the DMSO-treated $Arnt^{fx/fx}$ mice ($p < 0.05$).

quantitative RT-PCR (Figs. 2C–F). In the livers of $Arnt^{fx/fx}$ mice treated with dioxin, *Cyp1a1*, *Cyp1a2*, *Cyp1b1*, and *Ahrr* mRNA levels were significantly increased compared with DMSO-treated $Arnt^{fx/fx}$ mice (Figs.2C–F). However, in the livers of $Arnt^{fx/fx}Cre^{alb}$ mice, induction levels of all DRE-driven genes were ~90% lower than those in $Arnt^{fx/fx}$ mice (*Cyp1a1*, 89.4%; *Cyp1a2*, 84.5%; *Cyp1b1*, 95.7%; *Ahrr*, 92.7%) (Figs. 2C–F). The decreases in the induction of these genes was also reflected in their protein levels and enzyme activities; i.e., increases of CYP1A1, CYP1A2, and CYP1B1 protein levels and elevation of EROD and MROD activities (i.e., CYP1A1 and CYP1A2 enzyme activities, respectively)

were not observed in the livers of dioxin-treated *Arnt*$^{fx/fx}$*Cre*^{alb} mice but increases were observed in dioxin-treated *Arnt*$^{fx/fx}$ mice (Figs. 2G–I).

The Arnt$^{fx/fx}$Cre^{alb} *Mice Do Not Show Dioxin-Induced Hepatocellular Damage*

To investigate the role of hepatocyte ARNT in dioxin-induced liver toxicity, we analyzed characteristic toxic end points of dioxin exposure in *Arnt*$^{fx/fx}$ and *Arnt*$^{fx/fx}$*Cre*^{alb} mice. A statistically significant increase in liver weights was observed in response to dioxin exposure in *Arnt*$^{fx/fx}$ mice but not in *Arnt*$^{fx/fx}$*Cre*^{alb} mice (Fig. 3A). In contrast to the resistance to dioxin-induced hepatomegaly in the liver of *Arnt*$^{fx/fx}$*Cre*^{alb} mice, thymus weights were similarly decreased in both dioxin-treated *Arnt*$^{fx/fx}$ and *Arnt*$^{fx/fx}$*Cre*^{alb} mice (Fig. 3B). The dioxin-treated *Arnt*$^{fx/fx}$ mice displayed significant elevation of ALT activity compared with DMSO-treated *Arnt*$^{fx/fx}$ mice (DMSO; 52.5 ± 18.7 U/L, dioxin; 1339.5 ± 425.0) (Fig. 3C), whereas a significant change in ALT activity was not observed in either DMSO- or dioxin-treated *Arnt*$^{fx/fx}$*Cre*^{alb} mice (DMSO; 81.2 ± 58.3 U/L, dioxin; 33.5 ± 3.0) (Fig. 3C). To investigate dioxin-induced hepatotoxicity in *Arnt*$^{fx/fx}$ and *Arnt*$^{fx/fx}$*Cre*^{alb} mice, we analyzed liver sections by employing H&E staining for general pathology and F4/80 immunostaining for monitoring infiltration of macrophages (Figs. 3D–E, Supplementary data 1–2). In H&E-stained liver sections of dioxin-treated *Arnt*$^{fx/fx}$ mice, severe hepatocellular hydropic degeneration (zone 2) and focal inflammations (zones 1–2), which consisted of macrophages, lymphocytes, and necrotic cells, were observed (Fig. 3D, Supplementary data 1). In contrast, no dioxin-induced histological changes were observed in liver sections of dioxin-treated *Arnt*$^{fx/fx}$*Cre*^{alb} mice (Fig. 3D, Supplementary data 1). In liver sections of dioxin-treated *Arnt*$^{fx/fx}$ mice, a number of F4/80-positive cells were observed, whereas few F4/80-positive cells were observed in dioxin-treated *Arnt*$^{fx/fx}$*Cre*^{alb} mice (Fig. 3E, Supplementary data 2). To assess dioxin-induced steatosis in liver, we also analyzed the liver sections with Oil Red O (Fig. 3F, Supplementary data 3). In liver sections of dioxin-treated *Arnt*$^{fx/fx}$ mice, a number of lipid droplets were observed, whereas the level of lipid accumulation was not significantly different among DMSO-treated *Arnt*$^{fx/fx}$, DMSO-treated *Arnt*$^{fx/fx}$*Cre*^{alb}, and dioxin-treated *Arnt*$^{fx/fx}$*Cre*^{alb} mice (Fig. 3F, Supplementary data 3).

DISCUSSION

The ARNT is a member of PAS protein family and acts as a dimeric partner for a number of PAS domain-containing proteins (e.g., AHR, AHRR [AHR repressor], HIF1-α, HIF-2α, HIF3-α and possibly SIM1 [single minded], and SIM2) (McIntosh *et al.*, 2010). These ARNT-dependent PAS protein dimers play central roles in normal development and physiological homeostasis (McIntosh *et al.*, 2010). In the adaptive metabolic pathway, the AHR-ARNT complex has been shown to form in response to agonist exposure and bind genomic DREs that drive the expression of genes encoding xenobiotic metabolizing enzymes (Hankinson, 1995; McIntosh *et al.*, 2010; Nebert and Gonzalez, 1987; Schmidt and Bradfield, 1996). Although the evidence to support a role for ARNT in adaptive metabolism of xenobiotics is clear, we are less certain about the role for ARNT in the toxic and developmental signaling pathways of the AHR. In this regard, AHR signaling pathways have been proposed that are ARNT independent (Ge and Elferink, 1998; Klinge *et al.*, 2000; Oesch-Bartlomowicz *et al.*, 2005; Puga *et al.*, 2000; Reiners and Clift, 1999; Seidel and Denison, 1999; Tian *et al.*, 1999; Vogel *et al.*, 2007; Weiss *et al.*, 2008), and we now know that paralogues of ARNT, such as ARNT2, exist within certain cell types and may serve as potentially relevant AHR partners for some receptor-mediated events *in vivo* (Dougherty and Pollenz, 2008; Hirose *et al.*, 1996). Therefore, to understand the role of ARNT in the toxicological aspects of AHR, we generated a mouse model where the ARNT protein could be selectively deleted from specific cell types, including hepatocytes. This model was generated in an effort to overcome the essential role for ARNT in HIF signaling and the endothelial signaling by the AHR that mediates hepatovascular development. By circumventing the essential developmental roles of ARNT from putative roles in AHR-mediated biology, we predicted that a viable mouse model could be generated for the study of dioxin toxicity in the developing and adult mouse.

It has been demonstrated previously that global deletion of the *Arnt* gene results in early embryonic lethality between days E9.5 and E10, apparently due to a failure of blood vessel development in the yolk sac and embryo (Kozak *et al.*, 1997; Maltepe *et al.*, 1997). This is widely interpreted as an indication that *Arnt* deletion leads to disruption of HIF-1α and HIF-2α signaling rather than the AHR signaling (Adelman *et al.*, 1999; Kozak *et al.*, 1997; Maltepe *et al.*, 1997; Tomita *et al.*, 2000; Yim *et al.*, 2006). This conclusion is based on the observation that the global *Hif-1α*, *Hif-2α*, and *Arnt* null mice display overlapping developmental phenotypes and similar embryonic lethality (Compernolle *et al.*, 2002; Iyer *et al.*, 1998; Kotch *et al.*, 1999; Peng *et al.*, 2000; Ryan *et al.*, 1998; Tian *et al.*, 1998). From a toxicological perspective, the essential nature of ARNT in mammalian development is a significant impediment to toxicological studies in the adult animal. This issue is particularly acute for studies into the role of ARNT in the AHR-mediated toxicology of dioxins and related compounds.

In our earlier attempt to circumvent the developmental requirement for ARNT, we created mice harboring a hypomorphic *Arnt* allele by inserting the *Neo* gene between exons 6 and 7 (Walisser *et al.*, 2004b). These mice expressed ~10% of the wild-type level of the ARNT protein in most tissues. The observation that these hypomorphs survived to adulthood with

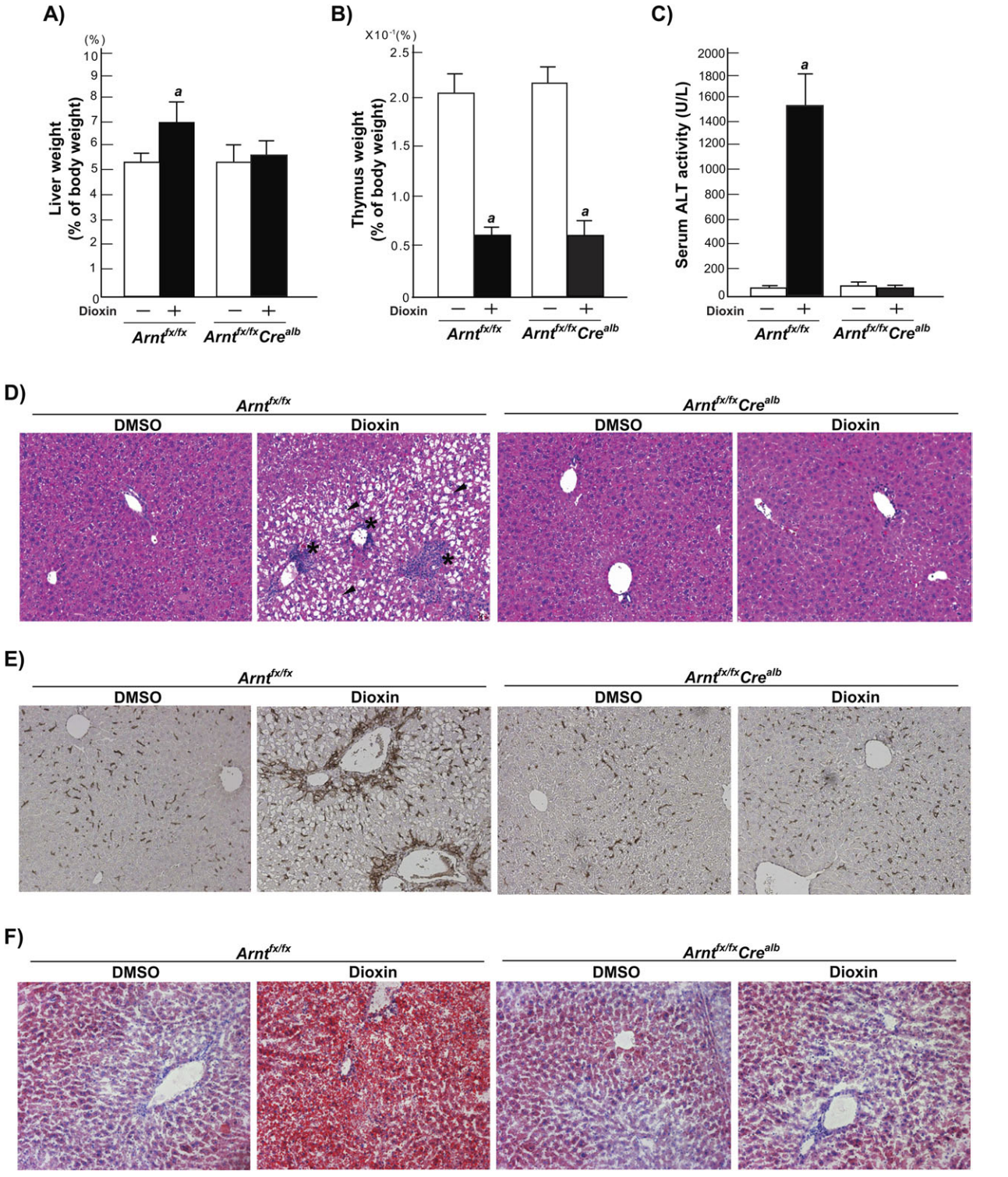

FIG. 3. Loss of dioxin-induced hepatotoxicity in *Arnt*$^{fx/fx}$*Cre*^{alb} mice. Mice were treated with DMSO vehicle alone or 100 μg/kg of dioxin in DMSO and sacrificed 7 days after the single ip injection. (A) Liver weight (% of total body weight), (B) thymus weight (% of total body weight) (C) serum ALT activity (units per liter). Each group contains four to six mice. Open bars, DMSO treatment; closed bars, dioxin treatment. Error bars represent SE a, significantly different relative to the DMSO-treated *Arnt*$^{fx/fx}$ mice ($p < 0.05$). (D–F) The liver sections were stained with H&E or Oil red O or immunostained with anti-F4/80 antibody. (D) H&E stain (magnification; ×100); black arrowhead, hydropic degenerations; *, focal inflammation. (E) F4/80 immunostain (magnification ×100); brown spots indicate F4/80-positive cells and (F) Oil Red O stain (magnification ×100); red spots indicate neutral lipids.

no overt pathology suggested that this hypomorphic model provided enough ARNT expression to allow sufficient HIF-1α and HIF-2α signaling and normal embryonic angiogenesis (Walisser *et al*., 2004b). The fact that these hypomorphic ARNT animals make it through early developmental angiogenesis, yet display a high frequency of patent DV, a phenocopy of the *Ahr* null mouse, leads us to propose that ARNT plays an essential role in AHR-mediated hepatovascular development (Harstad *et al*., 2006; Lahvis *et al*., 2000). These earlier data with the hypomorphic *Arnt* allele are also consistent with the idea that AHR-mediated hepatovascular development is more sensitive to the lower concentration of cellular ARNT protein than is HIF-1α- and HIF-2α-mediated embryonic angiogenesis (Walisser *et al*., 2004b).

The hypomorphic *Arnt* allele also provided some initial insight into AHR-mediated dioxin toxicity and the role that ARNT plays in this process (Walisser *et al*., 2004b). In the earlier study, we observed that the globally hypomorphic ARNT mice displayed resistance to common dioxin-induced toxic end points, such as thymic involution and hepatic injury, whereas the induction levels of CYP1A1/CYP1A2 enzyme activities were not significantly different between the hypomorphic ARNT and wild-type mice (Walisser *et al*., 2004b). This observation is consistent with the idea that many aspects of dioxin toxicity are uncoupled from induction of CYP1-dependent monooxygenases (Nukaya *et al*., 2009). Unfortunately, the hypomorphic ARNT mouse has a number of limitations. For example, the ARNT hypomorphic model does have significantly altered hepatic perfusion and smaller livers because of the high penetrance of patent DV in this model. Moreover, one has to consider the potential consequences of altered hypoxia signal transduction in this model that may be occurring globally even though they are undetected by gross measures of animal physiology, such as embryo survival rates and gross organ weights. Therefore, we turned our attention to the development of a hepatocyte-specific deletion of the ARNT protein as a way to more clearly demonstrate the role of ARNT in dioxin liver toxicity.

Given our prior observation that hepatocyte deletion of the *Ahr* did not influence vascular development, we predicted that the hepatocyte-*Arnt* deletion would yield an animal model with normal hepatovascular development and normal hepatic perfusion of xenobiotics-like dioxin (Walisser *et al*., 2005). In keeping with this prediction, our hepatocyte-*Arnt* null model displays normal DV closure and liver lobe morphology (Harstad *et al*., 2006). We interpret these data to indicate that the issues of embryonic development and hepatovascular development observed in global *Arnt* null and global *Arnt* hypomorphic models have been circumvented by selective deletion of ARNT in hepatocytes (Table 1). The normal birth rate of our conditional model is also evidence that ARNT in hepatocytes is not essential for normal HIF-1α- or HIF-2α-mediated embryonic angiogenesis or the AHR-mediated hepatovascular development.

The primary use of this hepatocyte-specific *Arnt* deletion mouse model was to provide a system to investigate the role of the ARNT protein in dioxin-induced liver toxicity. We observed that in response to acute dioxin exposure, hepatocyte-specific *Arnt* null mice are resistant to induced liver toxicity (i.e., no significant hepatomegaly, hepatic injury, hepatic inflammation, hydropic degeneration, or steatosis) and also resistant to the upregulation of the adaptive metabolic response (i.e., *Cyp1a1*, *Cyp1a2*, *Cyp1b1*, and *Ahrr*) (Figs. 2–3). These results demonstrate that ARNT in hepatocytes plays an essential role in the both AHR-mediated upregulation of adaptive xenobiotic metabolism and dioxin-induced hepatotoxicity. These data are consistent with results from a similar conditional model of ARNT expression, where ARNT deletion in T cells protects from the thymic toxicity of dioxin (Tomita *et al*., 2003). Coupled to previous work with hepatocyte-*Ahr* null mice (Walisser *et al*., 2005), these results demonstrate that the dioxin-induced adaptive metabolism and hepatotoxicity require both the AHR and the ARNT and are consistent with a model where the AHR-ARNT dimer driving expression of DRE-driven genes lies at the heart of acute hepatotoxic end points. By extension, these data argue against a role for hepatotoxic mechanisms that work through ARNT-independent mechanisms (Ge and Elferink, 1998; Klinge *et al*., 2000; Oesch-Bartlomowicz *et al*., 2005; Puga *et al*., 2000; Reiners and Clift, 1999; Seidel and Denison, 1999; Tian *et al*., 1999; Vogel *et al*., 2007; Weiss *et al*., 2008).

Our mouse model is similar in construction to that previously reported by others to investigate AHR-mediated adaptive metabolism and HIF-mediated liver gluconeogenesis/lipogenesis (Tomita *et al*., 2000; Wang *et al*., 2009). Although there are many similarities, there are also some important distinctions between our models. In our hepatocyte excision model, we begin with a genetic construct where the *Neo* cassette has been removed from the murine genome using recombination (Walisser *et al*., 2005). In the earlier model, *Neo* is left intact and may be causing some degree of *Arnt* hypomorphism and possibly even a high background of patent DV in the controls for those models (Walisser et al., 2004b). Given the potential influence of the DV on first pass clearance, we argue that excision of *Neo* is an important consideration in pharmacology studies employing recombinant alleles of AHR-ARNT signaling pathway factors.

Conclusions

We have generated a hepatocyte-specific *Arnt* null mouse model, which circumvents the issue of embryonic lethality observed in the global *Arnt* null mice and of hepatic vascular defect observed in hypomorphic *Arnt* mice. The hepatocyte-*Arnt* null mouse model displays disruption of adaptive upregulation of AHR-driven genes and little if any dioxin-induced hepatotoxicity. These results are consistent with similar observations from hepatocyte-specific *Ahr* null mice and demonstrate that both the AHR and the ARNT in

hepatocytes are essential for the majority of adaptive upregulation and dioxin-induced toxicity in liver. In future studies, this conditional *Arnt* mouse model can also be a powerful tool to understand the biological and cell-autonomous roles of ARNT-dependent signaling, such as HIFs, SIMs, and MOPs (member of PAS superfamily).

SUPPLEMENTARY DATA

Supplementary data are available online at http://toxsci.oxfordjournals.org/.

FUNDING

National Institutes of Health (R01-ES-06883, R37-ES-05703, T32-CA-009135, P30-CA-014520, and K08-ES-017283).

REFERENCES

Adelman, D. M., Maltepe, E., and Simon, M. C. (1999). Multilineage embryonic hematopoiesis requires hypoxic ARNT activity. *Genes Dev.* **13,** 2478–2483.

Bunger, M. K., Glover, E., Moran, S. M., Walisser, J. A., Lahvis, G. P., Hsu, E. L., and Bradfield, C. A. (2008). Abnormal liver development and resistance to 2,3,7,8-tetrachlorodibenzo-*p*-dioxin toxicity in mice carrying a mutation in the DNA-binding domain of the aryl hydrocarbon receptor. *Toxicol. Sci.* **106,** 83–92.

Bunger, M. K., Moran, S. M., Glover, E., Thomae, T. L., Lahvis, G. P., Lin, B. C., and Bradfield, C. A. (2003). Resistance to 2,3,7,8-tetrachlorodibenzo-*p*-dioxin toxicity and abnormal liver development in mice carrying a mutation in the nuclear localization sequence of the aryl hydrocarbon receptor. *J. Biol. Chem.* **278,** 17767–17774.

Compernolle, V., Brusselmans, K., Acker, T., Hoet, P., Tjwa, M., Beck, H., Plaisance, S., Dor, Y., Keshet, E., Lupu, F., *et al.* (2002). Loss of HIF-2alpha and inhibition of VEGF impair fetal lung maturation, whereas treatment with VEGF prevents fatal respiratory distress in premature mice. *Nat. Med.* **8,** 702–710.

Dougherty, E. J., and Pollenz, R. S. (2008). Analysis of Ah receptor-ARNT and Ah receptor-ARNT2 complexes in vitro and in cell culture. *Toxicol. Sci.* **103,** 191–206.

Ge, N. L., and Elferink, C. J. (1998). A direct interaction between the aryl hydrocarbon receptor and retinoblastoma protein. Linking dioxin signaling to the cell cycle. *J. Biol. Chem.* **273,** 22708–22713.

Hankinson, O. (1995). The aryl hydrocarbon receptor complex. *Annu. Rev. Pharmacol. Toxicol.* **35,** 307–340.

Harstad, E. B., Guite, C. A., Thomae, T. L., and Bradfield, C. A. (2006). Liver deformation in Ahr-null mice: evidence for aberrant hepatic perfusion in early development. *Mol. Pharmacol.* **69,** 1534–1541.

Hirose, K., Morita, M., Ema, M., Mimura, J., Hamada, H., Fujii, H., Saijo, Y., Gotoh, O., Sogawa, K., and Fujii-Kuriyama, Y. (1996). cDNA cloning and tissue-specific expression of a novel basic helix-loop-helix/PAS factor (Arnt2) with close sequence similarity to the aryl hydrocarbon receptor nuclear translocator (Arnt). *Mol. Cell. Biol.* **16,** 1706–1713.

Iyer, N. V., Kotch, L. E., Agani, F., Leung, S. W., Laughner, E., Wenger, R. H., Gassmann, M., Gearhart, J. D., Lawler, A. M., Yu, A. Y., *et al.* (1998). Cellular and developmental control of O2 homeostasis by hypoxia-inducible factor 1 alpha. *Genes Dev.* **12,** 149–162.

Klinge, C. M., Kaur, K., and Swanson, H. I. (2000). The aryl hydrocarbon receptor interacts with estrogen receptor alpha and orphan receptors COUP-TFI and ERRalpha1. *Arch. Biochem. Biophys.* **373,** 163–174.

Kotch, L. E., Iyer, N. V., Laughner, E., and Semenza, G. L. (1999). Defective vascularization of HIF-1alpha-null embryos is not associated with VEGF deficiency but with mesenchymal cell death. *Dev. Biol.* **209,** 254–267.

Kozak, K. R., Abbott, B., and Hankinson, O. (1997). ARNT-deficient mice and placental differentiation. *Dev. Biol.* **191,** 297–305.

Lahvis, G. P., Lindell, S. L., Thomas, R. S., McCuskey, R. S., Murphy, C., Glover, E., Bentz, M., Southard, J., and Bradfield, C. A. (2000). Portosystemic shunting and persistent fetal vascular structures in aryl hydrocarbon receptor-deficient mice. *Proc. Natl. Acad. Sci. U.S.A.* **97,** 10442–10447.

Lakso, M., Pichel, J. G., Gorman, J. R., Sauer, B., Okamoto, Y., Lee, E., Alt, F. W., and Westphal, H. (1996). Efficient in vivo manipulation of mouse genomic sequences at the zygote stage. *Proc. Natl. Acad. Sci. U.S.A.* **93,** 5860–5865.

Maltepe, E., Schmidt, J. V., Baunoch, D., Bradfield, C. A., and Simon, M. C. (1997). Abnormal angiogenesis and responses to glucose and oxygen deprivation in mice lacking the protein ARNT. *Nature* **386,** 403–407.

McIntosh, B. E., Hogenesch, J. B., and Bradfield, C. A. (2010). Mammalian Per-Arnt-Sim proteins in environmental adaptation. *Annu. Rev. Physiol.* **17,** 625–645.

Nebert, D. W., and Gonzalez, F. J. (1987). P450 genes: structure, evolution, and regulation. *Annu. Rev. Biochem.* **56,** 945–993.

Nukaya, M., Moran, S., and Bradfield, C. A. (2009). The role of the dioxin-responsive element cluster between the *Cyp1a1* and *Cyp1a2* loci in aryl hydrocarbon receptor biology. *Proc. Natl. Acad. Sci. U.S.A.* **106,** 4923–4928.

Oesch-Bartlomowicz, B., Huelster, A., Wiss, O., Antoniou-Lipfert, P., Dietrich, C., Arand, M., Weiss, C., Bockamp, E., and Oesch, F. (2005). Aryl hydrocarbon receptor activation by cAMP vs. dioxin: divergent signaling pathways. *Proc. Natl. Acad. Sci. U.S.A.* **102,** 9218–9223.

Peng, J., Zhang, L., Drysdale, L., and Fong, G. H. (2000). The transcription factor EPAS-1/hypoxia-inducible factor 2alpha plays an important role in vascular remodeling. *Proc. Natl. Acad. Sci. U.S.A.* **97,** 8386–8391.

Pohjanvirta, R., and Tuomisto, J. (1994). Short-term toxicity of 2,3,7,8-tetrachlorodibenzo-*p*-dioxin in laboratory animals: effects, mechanisms, and animal models. *Pharmacol. Rev.* **46,** 483–549.

Postic, C., Shiota, M., Niswender, K. D., Jetton, T. L., Chen, Y., Moates, J. M., Shelton, K. D., Lindner, J., Cherrington, A. D., and Magnuson, M. A. (1999). Dual roles for glucokinase in glucose homeostasis as determined by liver and pancreatic beta cell-specific gene knock-outs using Cre recombinase. *J. Biol. Chem.* **274,** 305–315.

Puga, A., Barnes, S. J., Dalton, T. P., Chang, C., Knudsen, E. S., and Maier, M. A. (2000). Aromatic hydrocarbon receptor interaction with the retinoblastoma protein potentiates repression of E2F-dependent transcription and cell cycle arrest. *J. Biol. Chem.* **275,** 2943–2950.

Reiners, J. J., Jr., and Clift, R. E. (1999). Aryl hydrocarbon receptor regulation of ceramide-induced apoptosis in murine hepatoma 1c1c7 cells. A function independent of aryl hydrocarbon receptor nuclear translocator. *J. Biol. Chem.* **274,** 2502–2510.

Ryan, H. E., Lo, J., and Johnson, R. S. (1998). HIF-1 alpha is required for solid tumor formation and embryonic vascularization. *EMBO J.* **17,** 3005–3015.

Savas, U., Bhattacharyya, K. K., Christou, M., Alexander, D. L., and Jefcoate, C. R. (1994). Mouse cytochrome P-450EF, representative of a new 1B subfamily of cytochrome P-450s. Cloning, sequence determination, and tissue expression. *J. Biol. Chem.* **269,** 14905–14911.

Schmidt, J. V., and Bradfield, C. A. (1996). Ah receptor signaling pathways. *Annu. Rev. Cell Dev. Biol.* **12,** 55–89.

Seidel, S. D., and Denison, M. S. (1999). Differential gene expression in wild-type and arnt-defective mouse hepatoma (Hepa1c1c7) cells. *Toxicol. Sci.* **52,** 217–225.

Tian, H., Hammer, R. E., Matsumoto, A. M., Russell, D. W., and McKnight, S. L. (1998). The hypoxia-responsive transcription factor EPAS1 is essential for catecholamine homeostasis and protection against heart failure during embryonic development. *Genes Dev.* **12,** 3320–3324.

Tian, Y., Ke, S., Denison, M. S., Rabson, A. B., and Gallo, M. A. (1999). Ah receptor and NF-kappaB interactions, a potential mechanism for dioxin toxicity. *J. Biol. Chem.* **274,** 510–515.

Tomita, S., Jiang, H. B., Ueno, T., Takagi, S., Tohi, K., Maekawa, S., Miyatake, A., Furukawa, A., Gonzalez, F. J., Takeda, J., *et al.* (2003). T cell-specific disruption of arylhydrocarbon receptor nuclear translocator (Arnt) gene causes resistance to 2,3,7,8-tetrachlorodibenzo-*p*-dioxin-induced thymic involution. *J. Immunol.* **171,** 4113–4120.

Tomita, S., Sinal, C. J., Yim, S. H., and Gonzalez, F. J. (2000). Conditional disruption of the aryl hydrocarbon receptor nuclear translocator (Arnt) gene leads to loss of target gene induction by the aryl hydrocarbon receptor and hypoxia-inducible factor 1alpha. *Mol. Endocrinol.* **14,** 1674–1681.

Vogel, C. F., Sciullo, E., Li, W., Wong, P., Lazennec, G., and Matsumura, F. (2007). RelB, a new partner of aryl hydrocarbon receptor-mediated transcription. *Mol. Endocrinol.* **21,** 2941–2955.

Walisser, J. A., Bunger, M. K., Glover, E., and Bradfield, C. A. (2004a). Gestational exposure of Ahr and Arnt hypomorphs to dioxin rescues vascular development. *Proc. Natl. Acad. Sci. U.S.A.* **101,** 16677–16682.

Walisser, J. A., Bunger, M. K., Glover, E., Harstad, E. B., and Bradfield, C. A. (2004b). Patent ductus venosus and dioxin resistance in mice harboring a hypomorphic Arnt allele. *J. Biol. Chem.* **279,** 16326–16331.

Walisser, J. A., Glover, E., Pande, K., Liss, A. L., and Bradfield, C. A. (2005). Aryl hydrocarbon receptor-dependent liver development and hepatotoxicity are mediated by different cell types. *Proc. Natl. Acad. Sci. U.S.A.* **102,** 17858–17863.

Wang, X. L., Suzuki, R., Lee, K., Tran, T., Gunton, J. E., Saha, A. K., Patti, M. E., Goldfine, A., Ruderman, N. B., Gonzalez, F. J., *et al.* (2009). Ablation of ARNT/HIF1beta in liver alters gluconeogenesis, lipogenic gene expression, and serum ketones. *Cell Metab.* **9,** 428–439.

Weiss, C., Faust, D., Schreck, I., Ruff, A., Farwerck, T., Melenberg, A., Schneider, S., Oesch-Bartlomowicz, B., Zatloukalová, J., Vondrácek, J., *et al.* (2008). TCDD deregulates contact inhibition in rat liver oval cells via Ah receptor, JunD and cyclin A. *Oncogene* **27,** 2198–2207.

Yim, S. H., Shah, Y., Tomita, S., Morris, H. D., Gavrilova, O., Lambert, G., Ward, J. M., and Gonzalez, F. J. (2006). Disruption of the Arnt gene in endothelial cells causes hepatic vascular defects and partial embryonic lethality in mice. *Hepatology* **44,** 550–560.